

# Measurement of the higher-order anisotropic flow coefficients for identified hadrons in Au+Au collisions at $\sqrt{s_{NN}} = 200$ GeV

- A. Adare,<sup>13</sup> S. Afanasiev,<sup>30</sup> C. Aidala,<sup>43, 44</sup> N.N. Ajitanand,<sup>62</sup> Y. Akiba,<sup>56, 57</sup> H. Al-Bataineh,<sup>50</sup> J. Alexander,<sup>62</sup> K. Aoki,<sup>35, 56</sup> Y. Aramaki,<sup>12</sup> E.T. Atomssa,<sup>36</sup> R. Averbeck,<sup>63</sup> T.C. Awes,<sup>52</sup> B. Azmoun,<sup>7</sup> V. Babintsev,<sup>24</sup> M. Bai,<sup>6</sup> G. Baksay,<sup>20</sup> L. Baksay,<sup>20</sup> K.N. Barish,<sup>8</sup> B. Bassalleck,<sup>49</sup> A.T. Basye,<sup>1</sup> S. Bathe,<sup>5, 8</sup> V. Baublis,<sup>55</sup> C. Baumann,<sup>45</sup> A. Bazilevsky,<sup>7</sup> S. Belikov,<sup>7, \*</sup> R. Belmont,<sup>67</sup> R. Bennett,<sup>63</sup> A. Berdnikov,<sup>59</sup> Y. Berdnikov,<sup>59</sup> A.A. Bickley,<sup>13</sup> J.S. Bok,<sup>50, 71</sup> K. Boyle,<sup>63</sup> M.L. Brooks,<sup>39</sup> H. Buesching,<sup>7</sup> V. Bumazhnov,<sup>24</sup> G. Bunce,<sup>7, 57</sup> S. Butsyk,<sup>39</sup> C.M. Camacho,<sup>39</sup> S. Campbell,<sup>63</sup> C.-H. Chen,<sup>63</sup> C.Y. Chi,<sup>14</sup> M. Chiu,<sup>7</sup> I.J. Choi,<sup>71</sup> R.K. Choudhury,<sup>4</sup> P. Christiansen,<sup>41</sup> T. Chujo,<sup>66</sup> P. Chung,<sup>62</sup> O. Chvala,<sup>8</sup> V. Cianciolo,<sup>52</sup> Z. Citron,<sup>63</sup> B.A. Cole,<sup>14</sup> M. Connors,<sup>63</sup> P. Constantin,<sup>39</sup> M. Csanad,<sup>18</sup> T. Cs org ,<sup>70</sup> T. Dahms,<sup>63</sup> S. Dairaku,<sup>35, 56</sup> I. Danchev,<sup>67</sup> K. Das,<sup>21</sup> A. Datta,<sup>43</sup> G. David,<sup>7</sup> A. Denisov,<sup>24</sup> A. Deshpande,<sup>57, 63</sup> E.J. Desmond,<sup>7</sup> O. Dietzsch,<sup>60</sup> A. Dion,<sup>63</sup> M. Donadelli,<sup>60</sup> O. Drapier,<sup>36</sup> A. Drees,<sup>63</sup> K.A. Drees,<sup>6</sup> J.M. Durham,<sup>39, 63</sup> A. Durum,<sup>24</sup> D. Dutta,<sup>4</sup> S. Edwards,<sup>21</sup> Y.V. Efremenko,<sup>52</sup> F. Ellinghaus,<sup>13</sup> T. Engelmore,<sup>14</sup> A. Enokizono,<sup>38</sup> H. En'yo,<sup>56, 57</sup> S. Esumi,<sup>66</sup> B. Fadem,<sup>46</sup> D.E. Fields,<sup>49</sup> M. Finger,<sup>9</sup> M. Finger, Jr.,<sup>9</sup> F. Fleuret,<sup>36</sup> S.L. Fokin,<sup>34</sup> Z. Fraenkel,<sup>69, \*</sup> J.E. Frantz,<sup>51, 63</sup> A. Franz,<sup>7</sup> A.D. Frawley,<sup>21</sup> K. Fujiwara,<sup>56</sup> Y. Fukao,<sup>56</sup> T. Fusayasu,<sup>48</sup> I. Garishvili,<sup>64</sup> A. Glenn,<sup>13</sup> H. Gong,<sup>63</sup> M. Gonin,<sup>36</sup> Y. Goto,<sup>56, 57</sup> R. Granier de Cassagnac,<sup>36</sup> N. Grau,<sup>2, 14</sup> S.V. Greene,<sup>67</sup> M. Grosse Perdekamp,<sup>25, 57</sup> T. Gunji,<sup>12</sup> H.-Å. Gustafsson,<sup>41, \*</sup> J.S. Haggerty,<sup>7</sup> K.I. Hahn,<sup>19</sup> H. Hamagaki,<sup>12</sup> J. Hamblen,<sup>64</sup> R. Han,<sup>54</sup> J. Hanks,<sup>14</sup> E.P. Hartouni,<sup>38</sup> E. Haslum,<sup>41</sup> R. Hayano,<sup>12</sup> X. He,<sup>22</sup> M. Heffner,<sup>38</sup> T.K. Hemmick,<sup>63</sup> T. Hester,<sup>8</sup> J.C. Hill,<sup>28</sup> M. Hohlmann,<sup>20</sup> W. Holzmann,<sup>14</sup> K. Homma,<sup>23</sup> B. Hong,<sup>33</sup> T. Horaguchi,<sup>23</sup> D. Hornback,<sup>64</sup> S. Huang,<sup>67</sup> T. Ichihara,<sup>56, 57</sup> R. Ichimiya,<sup>56</sup> J. Ide,<sup>46</sup> Y. Ikeda,<sup>66</sup> K. Imai,<sup>29, 35, 56</sup> M. Inaba,<sup>66</sup> D. Isenhower,<sup>1</sup> M. Ishihara,<sup>56</sup> T. Isobe,<sup>12, 56</sup> M. Issah,<sup>67</sup> A. Isupov,<sup>30</sup> D. Ivanischev,<sup>55</sup> B.V. Jacak,<sup>63</sup> J. Jia,<sup>7, 62</sup> J. Jin,<sup>14</sup> B.M. Johnson,<sup>7</sup> K.S. Joo,<sup>47</sup> D. Jouan,<sup>53</sup> D.S. Jumper,<sup>1</sup> F. Kajihara,<sup>12</sup> S. Kametani,<sup>56</sup> N. Kamihara,<sup>57</sup> J. Kamin,<sup>63</sup> J.H. Kang,<sup>71</sup> J. Kapustinsky,<sup>39</sup> K. Karatsu,<sup>35, 56</sup> D. Kawall,<sup>43, 57</sup> M. Kawashima,<sup>56, 58</sup> A.V. Kazantsev,<sup>34</sup> T. Kempel,<sup>28</sup> A. Khanzadeev,<sup>55</sup> K.M. Kijima,<sup>23</sup> B.I. Kim,<sup>33</sup> D.H. Kim,<sup>47</sup> D.J. Kim,<sup>31</sup> E. Kim,<sup>61</sup> E.-J. Kim,<sup>10</sup> S.H. Kim,<sup>71</sup> Y.-J. Kim,<sup>25</sup> E. Kinney,<sup>13</sup> K. Kiriluk,<sup>13</sup>  . Kiss,<sup>18</sup> E. Kistenev,<sup>7</sup> L. Kochenda,<sup>55</sup> B. Komkov,<sup>55</sup> M. Konno,<sup>66</sup> J. Koster,<sup>25</sup> D. Kotchetkov,<sup>49</sup> A. Kozlov,<sup>69</sup> A. Kr l,<sup>15</sup> A. Kravitz,<sup>14</sup> G.J. Kunde,<sup>39</sup> K. Kurita,<sup>56, 58</sup> M. Kurosawa,<sup>56</sup> Y. Kwon,<sup>71</sup> G.S. Kyle,<sup>50</sup> R. Lacev,<sup>62</sup> Y.S. Lai,<sup>14</sup> J.G. Lajoie,<sup>28</sup> A. Lebedev,<sup>28</sup> D.M. Lee,<sup>39</sup> J. Lee,<sup>19</sup> K. Lee,<sup>61</sup> K.B. Lee,<sup>33</sup> K.S. Lee,<sup>33</sup> M.J. Leitch,<sup>39</sup> M.A.L. Leite,<sup>60</sup> E. Leitner,<sup>67</sup> B. Lenzi,<sup>60</sup> X. Li,<sup>11</sup> P. Liebing,<sup>57</sup> L.A. Linden Levy,<sup>13</sup> T. Li ka,<sup>15</sup> A. Litvinenko,<sup>30</sup> H. Liu,<sup>39, 50</sup> M.X. Liu,<sup>39</sup> B. Love,<sup>67</sup> R. Luechtenborg,<sup>45</sup> D. Lynch,<sup>7</sup> C.F. Maguire,<sup>67</sup> Y.I. Makdisi,<sup>6</sup> A. Malakhov,<sup>30</sup> M.D. Malik,<sup>49</sup> V.I. Manko,<sup>34</sup> E. Mannel,<sup>14</sup> Y. Mao,<sup>54, 56</sup> H. Masui,<sup>66</sup> F. Matathias,<sup>14</sup> M. McCumber,<sup>63</sup> P.L. McGaughey,<sup>39</sup> N. Means,<sup>63</sup> B. Meredith,<sup>25</sup> Y. Miake,<sup>66</sup> A.C. Mignerey,<sup>42</sup> P. Mike ,<sup>9, 27</sup> K. Miki,<sup>56, 66</sup> A. Milov,<sup>7</sup> M. Mishra,<sup>3</sup> J.T. Mitchell,<sup>7</sup> S. Mizuno,<sup>56, 66</sup> A.K. Mohanty,<sup>4</sup> Y. Morino,<sup>12</sup> A. Morreale,<sup>8</sup> D.P. Morrison,<sup>7,  </sup> T.V. Moukhanova,<sup>34</sup> J. Murata,<sup>56, 58</sup> S. Nagamiya,<sup>32, 56</sup> J.L. Nagle,<sup>13,  </sup> M. Naglis,<sup>69</sup> M.I. Nagy,<sup>18</sup> I. Nakagawa,<sup>56, 57</sup> Y. Nakamiya,<sup>23</sup> T. Nakamura,<sup>32</sup> K. Nakano,<sup>56, 65</sup> J. Newby,<sup>38</sup> M. Nguyen,<sup>63</sup> R. Nouicer,<sup>7</sup> A.S. Nyanin,<sup>34</sup> E. O'Brien,<sup>7</sup> S.X. Oda,<sup>12</sup> C.A. Ogilvie,<sup>28</sup> M. Oka,<sup>66</sup> K. Okada,<sup>57</sup> Y. Onuki,<sup>56</sup> A. Oskarsson,<sup>41</sup> M. Ouchida,<sup>23, 56</sup> K. Ozawa,<sup>12</sup> R. Pak,<sup>7</sup> V. Pantuev,<sup>26, 63</sup> V. Papavassiliou,<sup>50</sup> I.H. Park,<sup>19</sup> J. Park,<sup>61</sup> S.K. Park,<sup>33</sup> W.J. Park,<sup>33</sup> S.F. Pate,<sup>50</sup> H. Pei,<sup>28</sup> J.-C. Peng,<sup>25</sup> H. Pereira,<sup>16</sup> V. Peresedov,<sup>30</sup> D.Yu. Peressounko,<sup>34</sup> C. Pinkenburg,<sup>7</sup> R.P. Pisani,<sup>7</sup> M. Proissl,<sup>63</sup> M.L. Purschke,<sup>7</sup> A.K. Purwar,<sup>39</sup> H. Qu,<sup>22</sup> J. Rak,<sup>31</sup> A. Rakotozafindrabe,<sup>36</sup> I. Ravinovich,<sup>69</sup> K.F. Read,<sup>52, 64</sup> K. Reygers,<sup>45</sup> D. Reynolds,<sup>62</sup> V. Riabov,<sup>55</sup> Y. Riabov,<sup>55</sup> E. Richardson,<sup>42</sup> D. Roach,<sup>67</sup> G. Roche,<sup>40</sup> S.D. Rolnick,<sup>8</sup> M. Rosati,<sup>28</sup> C.A. Rosen,<sup>13</sup> S.S.E. Rosendahl,<sup>41</sup> P. Rosnet,<sup>40</sup> P. Rukoyatkin,<sup>30</sup> P. Ru  ka,<sup>27</sup> B. Sahlmueller,<sup>45, 63</sup> N. Saito,<sup>32</sup> T. Sakaguchi,<sup>7</sup> K. Sakashita,<sup>56, 65</sup> V. Samsonov,<sup>55</sup> S. Sano,<sup>12, 68</sup> T. Sato,<sup>66</sup> S. Sawada,<sup>32</sup> K. Sedgwick,<sup>8</sup> J. Seele,<sup>13</sup> R. Seidl,<sup>25</sup> A.Yu. Semenov,<sup>28</sup> R. Seto,<sup>8</sup> D. Sharma,<sup>69</sup> I. Shein,<sup>24</sup> T.-A. Shibata,<sup>56, 65</sup> K. Shigaki,<sup>23</sup> M. Shimomura,<sup>66</sup> K. Shoji,<sup>35, 56</sup> P. Shukla,<sup>4</sup> A. Sickles,<sup>7</sup> C.L. Silva,<sup>60</sup> D. Silvermyr,<sup>52</sup> C. Silvestre,<sup>16</sup> K.S. Sim,<sup>33</sup> B.K. Singh,<sup>3</sup> C.P. Singh,<sup>3</sup> V. Singh,<sup>3</sup> M. Slune ka,<sup>9</sup> R.A. Soltz,<sup>38</sup> W.E. Sondheim,<sup>39</sup> S.P. Sorensen,<sup>64</sup> I.V. Sourikova,<sup>7</sup> N.A. Sparks,<sup>1</sup> P.W. Stankus,<sup>52</sup> E. Stenlund,<sup>41</sup> S.P. Stoll,<sup>7</sup> T. Sugitate,<sup>23</sup> A. Sukhanov,<sup>7</sup> J. Sziklai,<sup>70</sup> E.M. Takagui,<sup>60</sup> A. Taketani,<sup>56, 57</sup> R. Tanabe,<sup>66</sup> Y. Tanaka,<sup>48</sup> K. Tanida,<sup>35, 56, 57</sup> M.J. Tannenbaum,<sup>7</sup> S. Tarafdar,<sup>3</sup> A. Taranenko,<sup>62</sup> P. Tarj n,<sup>17</sup> H. Themann,<sup>63</sup> T.L. Thomas,<sup>49</sup> T. Todoroki,<sup>56, 66</sup> M. Togawa,<sup>35, 56</sup> A. Toia,<sup>63</sup> L. Tom  ek,<sup>27</sup> H. Torii,<sup>23</sup> R.S. Towell,<sup>1</sup> I. Tserruya,<sup>69</sup> Y. Tsuchimoto,<sup>23</sup> C. Vale,<sup>7, 28</sup> H. Valle,<sup>67</sup> H.W. van Hecke,<sup>39</sup> E. Vazquez-Zambrano,<sup>14</sup> A. Veicht,<sup>25</sup> J. Velkovska,<sup>67</sup> R. V  rtesi,<sup>17, 70</sup> A.A. Vinogradov,<sup>34</sup> M. Virius,<sup>15</sup>

V. Vrba,<sup>27</sup> E. Vznuzdaev,<sup>55</sup> X.R. Wang,<sup>50</sup> D. Watanabe,<sup>23</sup> K. Watanabe,<sup>66</sup> Y. Watanabe,<sup>56, 57</sup> F. Wei,<sup>28</sup> R. Wei,<sup>62</sup> J. Wessels,<sup>45</sup> S.N. White,<sup>7</sup> D. Winter,<sup>14</sup> J.P. Wood,<sup>1</sup> C.L. Woody,<sup>7</sup> R.M. Wright,<sup>1</sup> M. Wysocki,<sup>13</sup> W. Xie,<sup>57</sup> Y.L. Yamaguchi,<sup>12</sup> K. Yamaura,<sup>23</sup> R. Yang,<sup>25</sup> A. Yanovich,<sup>24</sup> J. Ying,<sup>22</sup> S. Yokkaichi,<sup>56, 57</sup> Z. You,<sup>54</sup> G.R. Young,<sup>52</sup> I. Younus,<sup>37, 49</sup> I.E. Yushmanov,<sup>34</sup> W.A. Zajc,<sup>14</sup> C. Zhang,<sup>52</sup> S. Zhou,<sup>11</sup> and L. Zolin<sup>30</sup>

(PHENIX Collaboration)

<sup>1</sup>Abilene Christian University, Abilene, Texas 79699, USA

<sup>2</sup>Department of Physics, Augustana College, Sioux Falls, South Dakota 57197, USA

<sup>3</sup>Department of Physics, Banaras Hindu University, Varanasi 221005, India

<sup>4</sup>Bhabha Atomic Research Centre, Bombay 400 085, India

<sup>5</sup>Baruch College, City University of New York, New York, New York, 10010 USA

<sup>6</sup>Collider-Accelerator Department, Brookhaven National Laboratory, Upton, New York 11973-5000, USA

<sup>7</sup>Physics Department, Brookhaven National Laboratory, Upton, New York 11973-5000, USA

<sup>8</sup>University of California - Riverside, Riverside, California 92521, USA

<sup>9</sup>Charles University, Ovocný trh 5, Praha 1, 116 36, Prague, Czech Republic

<sup>10</sup>Chonbuk National University, Jeonju, 561-756, Korea

<sup>11</sup>Science and Technology on Nuclear Data Laboratory, China Institute of Atomic Energy, Beijing 102413, People's Republic of China

<sup>12</sup>Center for Nuclear Study, Graduate School of Science, University of Tokyo, 7-3-1 Hongo, Bunkyo, Tokyo 113-0033, Japan

<sup>13</sup>University of Colorado, Boulder, Colorado 80309, USA

<sup>14</sup>Columbia University, New York, New York 10027 and Nevis Laboratories, Irvington, New York 10533, USA

<sup>15</sup>Czech Technical University, Zikova 4, 166 36 Prague 6, Czech Republic

<sup>16</sup>Dapnia, CEA Saclay, F-91191, Gif-sur-Yvette, France

<sup>17</sup>Debrecen University, H-4010 Debrecen, Egyetem tér 1, Hungary

<sup>18</sup>ELTE, Eötvös Loránd University, H-1117 Budapest, Pázmány Péter sétány 1/A, Hungary

<sup>19</sup>Ewha Womans University, Seoul 120-750, Korea

<sup>20</sup>Florida Institute of Technology, Melbourne, Florida 32901, USA

<sup>21</sup>Florida State University, Tallahassee, Florida 32306, USA

<sup>22</sup>Georgia State University, Atlanta, Georgia 30303, USA

<sup>23</sup>Hiroshima University, Kagamiyama, Higashi-Hiroshima 739-8526, Japan

<sup>24</sup>IHEP Protvino, State Research Center of Russian Federation, Institute for High Energy Physics, Protvino, 142281, Russia

<sup>25</sup>University of Illinois at Urbana-Champaign, Urbana, Illinois 61801, USA

<sup>26</sup>Institute for Nuclear Research of the Russian Academy of Sciences, prospekt 60-letiya Oktyabrya 7a, Moscow 117312, Russia

<sup>27</sup>Institute of Physics, Academy of Sciences of the Czech Republic, Na Slovance 2, 182 21 Prague 8, Czech Republic

<sup>28</sup>Iowa State University, Ames, Iowa 50011, USA

<sup>29</sup>Advanced Science Research Center, Japan Atomic Energy Agency, 2-4

Shirakata Shirane, Tokai-mura, Naka-gun, Ibaraki-ken 319-1195, Japan

<sup>30</sup>Joint Institute for Nuclear Research, 141980 Dubna, Moscow Region, Russia

<sup>31</sup>Helsinki Institute of Physics and University of Jyväskylä, P.O.Box 35, FI-40014 Jyväskylä, Finland

<sup>32</sup>KEK, High Energy Accelerator Research Organization, Tsukuba, Ibaraki 305-0801, Japan

<sup>33</sup>Korea University, Seoul, 136-701, Korea

<sup>34</sup>Russian Research Center "Kurchatov Institute," Moscow, 123098 Russia

<sup>35</sup>Kyoto University, Kyoto 606-8502, Japan

<sup>36</sup>Laboratoire Leprince-Ringuet, Ecole Polytechnique, CNRS-IN2P3, Route de Saclay, F-91128, Palaiseau, France

<sup>37</sup>Physics Department, Lahore University of Management Sciences, Lahore 54792, Pakistan

<sup>38</sup>Lawrence Livermore National Laboratory, Livermore, California 94550, USA

<sup>39</sup>Los Alamos National Laboratory, Los Alamos, New Mexico 87545, USA

<sup>40</sup>LPC, Université Blaise Pascal, CNRS-IN2P3, Clermont-Fd, 63177 Aubiere Cedex, France

<sup>41</sup>Department of Physics, Lund University, Box 118, SE-221 00 Lund, Sweden

<sup>42</sup>University of Maryland, College Park, Maryland 20742, USA

<sup>43</sup>Department of Physics, University of Massachusetts, Amherst, Massachusetts 01003-9337, USA

<sup>44</sup>Department of Physics, University of Michigan, Ann Arbor, Michigan 48109-1040, USA

<sup>45</sup>Institut für Kernphysik, University of Muenster, D-48149 Muenster, Germany

<sup>46</sup>Muhlenberg College, Allentown, Pennsylvania 18104-5586, USA

<sup>47</sup>Myongji University, Yongin, Kyonggi-do 449-728, Korea

<sup>48</sup>Nagasaki Institute of Applied Science, Nagasaki-shi, Nagasaki 851-0193, Japan

<sup>49</sup>University of New Mexico, Albuquerque, New Mexico 87131, USA

<sup>50</sup>New Mexico State University, Las Cruces, New Mexico 88003, USA

<sup>51</sup>Department of Physics and Astronomy, Ohio University, Athens, Ohio 45701, USA

<sup>52</sup>Oak Ridge National Laboratory, Oak Ridge, Tennessee 37831, USA

<sup>53</sup>IPN-Orsay, Université Paris Sud, CNRS-IN2P3, BP1, F-91406, Orsay, France

<sup>54</sup>Peking University, Beijing 100871, People's Republic of China

<sup>55</sup>PNPI, Petersburg Nuclear Physics Institute, Gatchina, Leningrad Region, 188300, Russia

- <sup>56</sup>RIKEN Nishina Center for Accelerator-Based Science, Wako, Saitama 351-0198, Japan  
<sup>57</sup>RIKEN BNL Research Center, Brookhaven National Laboratory, Upton, New York 11973-5000, USA  
<sup>58</sup>Physics Department, Rikkyo University, 3-34-1 Nishi-Ikebukuro, Toshima, Tokyo 171-8501, Japan  
<sup>59</sup>Saint Petersburg State Polytechnic University, St. Petersburg, 195251 Russia  
<sup>60</sup>Universidade de São Paulo, Instituto de Física, Caixa Postal 66318, São Paulo CEP05315-970, Brazil  
<sup>61</sup>Department of Physics and Astronomy, Seoul National University, Seoul 151-742, Korea  
<sup>62</sup>Chemistry Department, Stony Brook University, SUNY, Stony Brook, New York 11794-3400, USA  
<sup>63</sup>Department of Physics and Astronomy, Stony Brook University, SUNY, Stony Brook, New York 11794-3800, USA  
<sup>64</sup>University of Tennessee, Knoxville, Tennessee 37996, USA  
<sup>65</sup>Department of Physics, Tokyo Institute of Technology, Oh-okayama, Meguro, Tokyo 152-8551, Japan  
<sup>66</sup>Institute of Physics, University of Tsukuba, Tsukuba, Ibaraki 305, Japan  
<sup>67</sup>Vanderbilt University, Nashville, Tennessee 37235, USA  
<sup>68</sup>Waseda University, Advanced Research Institute for Science and Engineering, 17 Kikui-cho, Shinjuku-ku, Tokyo 162-0044, Japan  
<sup>69</sup>Weizmann Institute, Rehovot 76100, Israel  
<sup>70</sup>Institute for Particle and Nuclear Physics, Wigner Research Centre for Physics, Hungarian Academy of Sciences (Wigner RCP, RMKI) H-1525 Budapest 114, POBox 49, Budapest, Hungary  
<sup>71</sup>Yonsei University, IPAP, Seoul 120-749, Korea

(Dated: September 27, 2018)

New PHENIX measurements of the anisotropic flow coefficients  $v_2\{\Psi_2\}$ ,  $v_3\{\Psi_3\}$ ,  $v_4\{\Psi_4\}$  and  $v_4\{\Psi_2\}$  for identified particles ( $\pi^\pm$ ,  $K^\pm$ , and  $p + \bar{p}$ ) obtained relative to the event planes  $\Psi_n$  in Au+Au collisions at  $\sqrt{s_{NN}} = 200$  GeV are presented as functions of collision centrality and particle transverse momenta  $p_T$ . The  $v_n$  coefficients show characteristic patterns consistent with hydrodynamical expansion of the matter produced in the collisions. For each harmonic  $n$ , a modified valence quark number  $n_q$  scaling plotting  $v_n/(n_q)^{n/2}$  versus  $KE_T/n_q$  is observed to yield a single curve for all the measured particle species for a broad range of transverse kinetic energies  $KE_T$ . A simultaneous blast wave model fit to the observed particle spectra and  $v_n(p_T)$  coefficients identifies spatial eccentricities  $s_n$  at freeze-out, which are much smaller than the initial-state geometric values.

PACS numbers: 25.75.Dw

The quark-gluon plasma (QGP) is a novel phase of nuclear matter at high temperature and energy density, whose existence is predicted by quantum chromodynamics (QCD) [1]. A wide variety of experimental observations at the Relativistic Heavy Ion Collider (RHIC) [2–5] provide strong evidence for the formation of a QGP in ultra-relativistic heavy ion collisions, particularly (i) the magnitude of the observed suppression of high  $p_T$  ( $p_T \gtrsim 10$  GeV/c) particles, relative to the scaled yield from  $p+p$  collisions; and (ii) the large azimuthal anisotropy or anisotropic flow of the low- $p_T$  ( $p_T \lesssim 3 - 4$  GeV/c) bulk of hadrons in the final state. The flow of low- $p_T$  particles has been attributed to anisotropic expansion of the QGP [6–8], and consequently the measured strength of anisotropic flow should be sensitive to the transport properties of the QGP and the mechanism for its space-time evolution.

The magnitude of anisotropic flow can be quantified by the Fourier coefficients  $v_n$  of the azimuthal distribution of produced particles [9, 10]

$$\frac{dN}{d\phi} \propto 1 + \sum_{n=1} 2v_n\{\Psi_n\} \cos(n(\phi - \Psi_n)), \quad (1)$$

where  $v_n\{\Psi_n\} = \langle \cos(n(\phi - \Psi_n)) \rangle$ ,  $n$  is the order of the harmonics,  $\phi$  is the azimuthal angle of the particles, and  $\Psi_n$  is the azimuthal angle of the  $n$ th order event plane. In early studies with symmetric systems,  $v_n$  was presumed

to be zero for odd  $n$  due to the assumption that initial-state energy densities were smooth and symmetric across the transverse plane. The recent observations of sizable  $v_n$  values for odd  $n$  [11–15] confirms the important role of fluctuations in the initial-state collision geometry [16].

Model-dependent analyses of the measurements for higher-order harmonics for inclusive hadrons measured in Au+Au and Pb+Pb collisions at RHIC and LHC have indicated that such measurements can provide simultaneous constraints for initial-state fluctuation models and the specific shear viscosity  $\eta/s$  (*i.e.* the ratio of shear viscosity  $\eta$  to entropy density  $s$ ) of the QGP [8, 11, 17–19]. We expect that the new data on higher-order  $v_n$  for identified particles presented here will provide more stringent constraints for  $\eta/s$  and the reaction dynamics, as well as to further differentiate among initial-state fluctuation models. Here, we show that our  $v_n$  measurements for different particle species provide (i) more demanding tests for the constituent quark number scaling and quark coalescence models [20–22] by extending our previously observed scaling for  $v_2$  [23, 24] to higher harmonics; and (ii) new insight on the expansion dynamics, as explored below with blast wave model fits [25–27].

The results presented here for Au+Au collisions at  $\sqrt{s_{NN}} = 200$  GeV are obtained with the PHENIX experiment from an analysis of  $4.14 \times 10^9$  minimum bias events taken during the 2007 running period. Collision central-

ity is obtained with the beam-beam counters (BBC) [28]. Charged hadrons are reconstructed in a pseudorapidity ( $\eta_p$ ) range of  $|\eta_p| < 0.35$  using the drift chamber (DC) and pad chamber (PC) subsystems [29]. The ring imaging Čerenkov counter (RICH) is employed to veto conversion electrons. The azimuthal angle coverage  $\Delta\varphi$  of PC, DC, and RICH are  $\Delta\varphi = \pi$  rad. Time-of-flight detectors in both the East (TOFE,  $\Delta\varphi = \pi/4$  rad) and West (TOFW,  $\Delta\varphi = 0.342$  rad) arms are used for  $\pi^\pm, K^\pm$ , and  $p + \bar{p}$  identification after the conversion electron veto [30]. The timing resolution of TOFE (TOFW) is 133 ( $84 \pm 1$ ) ps. For  $p_T < 3$  GeV/c both TOFE and TOFW detectors were used and a purity of greater than 98% was achieved for particle identification. For  $p_T > 3$  GeV/c only TOFW was used, employing the additional information of Čerenkov response by  $K^\pm$  and  $p + \bar{p}$  in the Aerogel Čerenkov Counter (ACC) detector which overlaps the  $\Delta\varphi = 0.171$  of TOFW acceptance; with this, particle purity of greater than 90% was also achieved for  $3 < p_T < 4$  GeV/c as detailed in [30]. The contamination from different hadrons are negligible in this analysis.

Measurements of the flow coefficients  $v_2\{\Psi_2\}$ ,  $v_3\{\Psi_3\}$ ,  $v_4\{\Psi_4\}$  and  $v_4\{\Psi_2\}$  as a function of centrality and  $p_T$  for  $\pi^\pm, K^\pm$ , and  $p + \bar{p}$  (*i.e.* with charge signs combined) are obtained with both the event-plane (EP) and the long-range two-particle correlation (2PC) methods.

In the EP method a measured event-plane direction  $\Psi_n^{\text{obs}}$  is determined for every event and for each order  $n$ , using two reaction plane hodoscopes RXN-N in the North and RXN-S in the South arms of the PHENIX experiment. They have 24 segments in each arm and cover  $1.0 < |\eta_p| < 2.8$  [31]. The  $\Psi_n^{\text{obs}}$  are determined by weighting the azimuthal angle  $\phi_i$  of each RXN element with its charge deposited by particles for that event as  $\tan(n\Psi_n^{\text{obs}}) = \sum_i w_i \sin(n\phi_i) / \sum_i w_i \cos(n\phi_i)$ . The flow magnitudes  $v_n\{\Psi_n\} = \langle \cos n(\phi - \Psi_n^{\text{obs}}) \rangle / \text{Res}\{n, \Psi_n\}$  are then measured with respect to each harmonic event plane, where  $\phi$  is the azimuthal angle of the hadron and  $\text{Res}\{n, \Psi_n\}$  is the event plane resolution. The latter is estimated using RXN S-N  $\Psi_n$  correlations  $\langle \cos n(\Psi_n^S - \Psi_n^N) \rangle$  as performed in Ref. [32–34]; in best  $\text{Res}\{2, \Psi_2\} \sim 0.75$  and  $\text{Res}\{4, \Psi_2\} \sim 0.5$  ( $\text{Res}\{3, \Psi_3\} \sim 0.3$  and  $\text{Res}\{4, \Psi_4\} \sim 0.15$ ) in 20%–30% (0%–10%) centrality bin.

The 2PC method pairs the hadrons with deposited charges in the RXN segments. The relative azimuthal angle of particle hits in separate  $\eta_p$  ranges  $A$  and  $B$ ,  $\Delta\phi \equiv \phi^A - \phi^B$ , reflects the products of the  $v_n$  via  $dN/d\Delta\phi \propto 1 + \sum_{n=1} 2v_n^A v_n^B \cos(n\Delta\phi)$  [33, 35, 36]. We analyze the  $\Delta\phi$  correlations using event mixing technique for two pair combinations;  $(A, B) = (\text{HAD}, \text{RXN})$  and  $(A, B) = (\text{RXN-N}, \text{RXN-S})$ . These correlations then fix the event-averaged products  $\langle v_n^{\text{HAD}} v_n^{\text{RXN}} \rangle$  and  $\langle v_n^{\text{RXN}} v_n^{\text{RXN}} \rangle$ , and allow us to obtain the  $v_n$  for hadrons as  $v_n^{\text{HAD}} = \langle v_n^{\text{HAD}} v_n^{\text{RXN}} \rangle / \sqrt{\langle v_n^{\text{RXN}} v_n^{\text{RXN}} \rangle}$ . Results in a

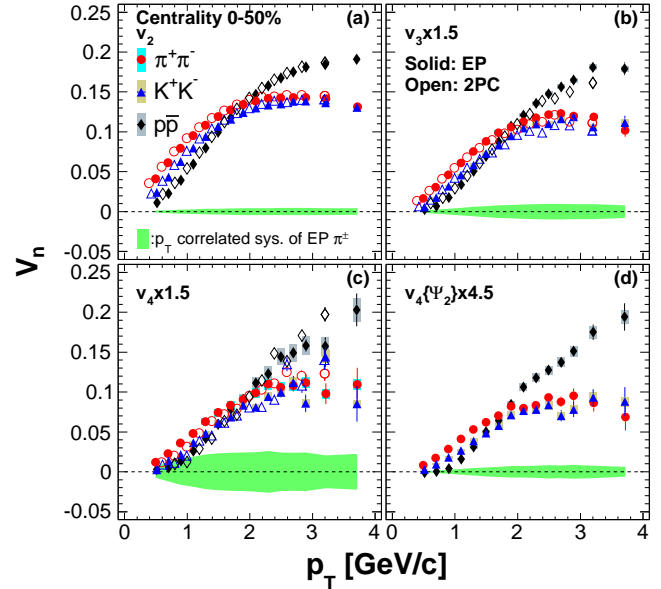


FIG. 1: (Color online) Fourier coefficients for charge combined  $\pi^\pm, K^\pm$ , and  $p + \bar{p}$  at midrapidity for 0%–50% central Au+Au collisions at  $\sqrt{s_{NN}} = 200$  GeV. The green bands indicate the  $p_T$ -correlated systematic uncertainties of the  $\pi^\pm$  results from the EP method. The shaded boxes around the data points are  $p_T$ -uncorrelated systematic uncertainties.

wide centrality range are obtained by integrating centrality differential measurements with their multiplicity weight [37].

The systematic uncertainties in the  $v_n$  measurements were estimated for: (*i*) EP resolution (correlated among  $v_n(p_T)$  for each hadron species with the same fraction); (*ii*) occupancy effects in the detector acceptance (correlated among  $v_n(p_T)$  for each hadron species with the same constant in the entire  $p_T$  range); (*iii*) hadron track reconstruction; and (*iv*) particle identification. The systematic uncertainties of (*i*)–(*ii*) are  $p_T$ -correlated and those of (*iii*)–(*iv*) are  $p_T$ -uncorrelated. Table I summarizes typical systematic sizes for  $\pi^\pm v_n$ .

TABLE I: Systematic uncertainties of  $\pi^\pm v_n$  at  $p_T = 2$  GeV/c in 0%–10% (30%–50%) central collisions. Uncertainties of the source (*ii*) are absolute; the others are relative.

Source	$v_2$	$v_3$	$v_4$	$v_4\{\Psi_2\}$
( <i>i</i> ) EP[%]	4.3(3.0)	4.7(12.5)	16(31)	34(7.0)
( <i>ii</i> ) Occupancy	0.005(0)	0(0)	0(0)	0(0)
( <i>iii</i> ) Tracking[%]	1.4(0.3)	0.7(1.0)	2.6(2.8)	7.7(1.7)
( <i>iv</i> ) PID[%]	3.1(1.0)	1.6(5.9)	4.8(6.8)	10.4(1.7)

Figures 1(a) - (c) show a comparison of  $v_2(p_T)$ ,  $v_3(p_T)$ , and  $v_4(p_T)$  for  $\pi^\pm, K^\pm$ , and  $p + \bar{p}$  for the EP (solid points) and 2PC (open points) methods in 0%–50% cen-

tral collisions; they indicate good agreement between the two methods of analysis. Shown in Fig. 1(d) is  $v_4\{\Psi_2\}$ , *i.e.*, the fourth harmonic coefficient with respect to the second harmonic event plane. It can be seen that  $v_4\{\Psi_2\}$  is smaller than  $v_4\{\Psi_4\}$  but still sizable, indicating significant correlations between  $\Psi_2$  and  $\Psi_4$  [38] as can be ascertained through the trigonometric identity  $v_4\{\Psi_2\}/v_4\{\Psi_4\} = \langle \cos 4(\Psi_2 - \Psi_4) \rangle$ .

There are two trends common to all the  $n = 2, 3, 4$  results shown in Fig. 1: (I) in the low- $p_T$  region the anisotropy appears largest for the lightest hadron and smallest for the heaviest hadron, reflecting the mass ordering from the common velocity field (*i.e.* radial flow); (II) in the intermediate- $p_T$  ( $3 \lesssim p_T \lesssim 4$  GeV/c) region this mass dependence partly reverses, such that the anisotropy is greater for the (anti-)baryons ( $n_q = 3$ ) than for the mesons ( $n_q = 2$ ) at the same  $p_T$ . The  $p_T$ -correlated systematic uncertainties do not negate the trends of (I) and (II). These patterns have been observed previously in  $v_2$  measurements for identified particles in Au+Au collisions at RHIC [27, 30], and are also seen here to hold for the higher moments  $v_3$ ,  $v_4$ , and  $v_4\{\Psi_2\}$ . The mass dependence in the low- $p_T$  range is a generic feature of hydrodynamical models, and the dependence on valence quark number in the intermediate- $p_T$  region has been associated with the development of flow in the partonic phase [23]. The persistence of these trends for all anisotropic moments  $n = 2, 3, 4$  suggests that all the measured orders of azimuthal anisotropy are driven by similar physics.

The  $v_n$  of  $\pi^\pm$ ,  $K^\pm$ , and  $p + \bar{p}$  measured with the event plane method are shown in Fig. 2 for the centrality selections 0%–10%, 10%–20%, 20%–30%, and 30%–50%. The same mass dependence of  $v_n$  is seen in the low- $p_T$  region for all harmonics and centralities. The evolution of baryon-meson splitting at intermediate- $p_T$  is also observed for all centralities in  $v_2$  and  $v_3$  but could not be confirmed for  $v_4$  in the most central and more peripheral events, or for  $v_4\{\Psi_2\}$  in the most central events due to the lower statistical significance of the measurements in those bins.

The baryon-meson splitting in the intermediate- $p_T$  region can be taken as an indication that the number of constituent valence quarks  $n_q$  is an important determinant of final-state hadron flow in this range. Indeed, the  $v_2$  data for identified hadrons had previously been seen to scale such that  $v_2/n_q$  was the same for different particle species when evaluated at the same transverse kinetic energy per constituent quark number  $KE_T/n_q \lesssim 1$  GeV ( $KE_T \equiv m_T - m_0$  and  $m_T \equiv \sqrt{p_T^2 + m_0^2}$ , where  $m_0$  is a hadron mass) *i.e.* “quark number scaling” [23, 30]. We have found that the present data obey a generalization of this scaling where, for each harmonic order  $n$ , the values of  $v_n/(n_q)^{n/2}$  vs.  $KE_T/n_q$  lie on a single curve for all the measured species within a ±15% range. The adherence of the data to this empirical scaling is shown in Fig. 3; it re-

fects the combination of the quark number scaling for  $v_2$  and the empirical observation of  $v_n(p_T) \propto (v_2)^{n/2}$  [13, 17] for charged hadrons, which may stem from the hydrodynamic evolution of the medium [9, 18, 39, 40], the quark coalescence process [41], and/or the acoustic nature of anisotropic flow [17].

The Blast Wave (BW) model [25–27] is a description of a fluid freeze-out state characterized by its temperature  $T_f$  and its radial flow rapidity  $\rho_0$ . Here we generalize the description to include azimuthal rapidity anisotropies  $\rho_n$  and spatial density anisotropies  $s_n$  for  $n = 2, 3, 4$ , where  $\rho(n, \phi, r)$  and  $S(n, \phi)$  are defined as  $\rho(n, \phi, r) = \rho_0(1 + 2\rho_n \cos(n\phi)) \times r/R_{\max}$  and  $S(n, \phi) = 1 + 2s_n \cos(n\phi)$ . The spectra and anisotropies of all hadrons freezing out of the fluid can then be predicted via

$$\frac{dN}{p_T dp_T} \propto \int r dr \int d\phi m_T I_0(\alpha_t) K_1(\beta_t) \\ v_n(p_T) = \frac{\int r dr \int d\phi \cos(n\phi) I_n(\alpha_t) K_1(\beta_t) S(n, \phi)}{\int r dr \int d\phi I_0(\alpha_t) K_1(\beta_t) S(n, \phi)}, \quad (2)$$

where  $I_n$  and  $K_1$  are modified Bessel functions of the first and second kind,  $\alpha_t = (p_T/T_f) \sinh \rho(n, \phi, r)$ , and  $\beta_t = (m_T/T_f) \cosh \rho(n, \phi, r)$ . Using single particle spectra from Ref. [42] together with the  $v_n$  data, BW parameters  $T_f$ ,  $\rho_0$ ,  $\rho_n$ , and  $s_n$  are extracted via simultaneous fitting of the  $\pi^\pm$ ,  $K^\pm$ , and  $p + \bar{p}$  data for  $KE_T < 1.0$  GeV with a minimization of global  $\chi^2$ , separately for each centrality selection and each order  $n$ .

The results for the BW parameters are shown in Fig. 4 and the fits to  $v_n(p_T)$  are compared to the data in Fig. 2. The freeze-out temperatures and radially averaged flow rapidities  $\langle \rho \rangle = \int [\rho_0 \times r/R_{\max}] r dr / \int r dr$  are in good agreement for the fits at different  $n$ , as would be required for a model of freeze-out. These two obtained parameters are consistent with the previous blast wave analysis of single particle spectra presented by PHENIX [43].

The radial rapidity and spatial density anisotropies  $\rho_n$  and  $s_n$  extracted from the fits are shown against the average initial-state spatial anisotropy  $\varepsilon_n\{\Psi_n\} = \langle \{r^2 \cos n(\phi^{\text{part}} - \Psi_n^{pp})\} / \{r^2\} \rangle$ , where  $r$  and  $\phi^{\text{part}}$  are the polar coordinate positions of collision participant nucleons defined by Glauber models [16, 44], and  $\Psi_n^{pp}$  is the participant-plane determined as  $\tan(n\Psi_n^{pp}) = \{r^2 \sin n\phi^{\text{part}}\} / \{r^2 \cos n\phi^{\text{part}}\}$ . Here, the brackets “⟨⟩” and “{ }” denote averages on events and participants. The amplitude of  $\varepsilon_n$  is smallest for most-central collisions and increases with centrality percentile. The  $\rho_n$  values generally track the  $\varepsilon_n$  on a common curve for  $n = 2, 3, 4$ . The spatial density anisotropies  $s_n$  also show an increasing trend, but with more variation. That is,  $s_3 < s_2$  in midcentral collisions, and  $s_4 = 0$  in relatively central collisions. These trends may indicate that hydrodynamic expansion from a given initial eccentricity results in essentially more quenching of the high-order

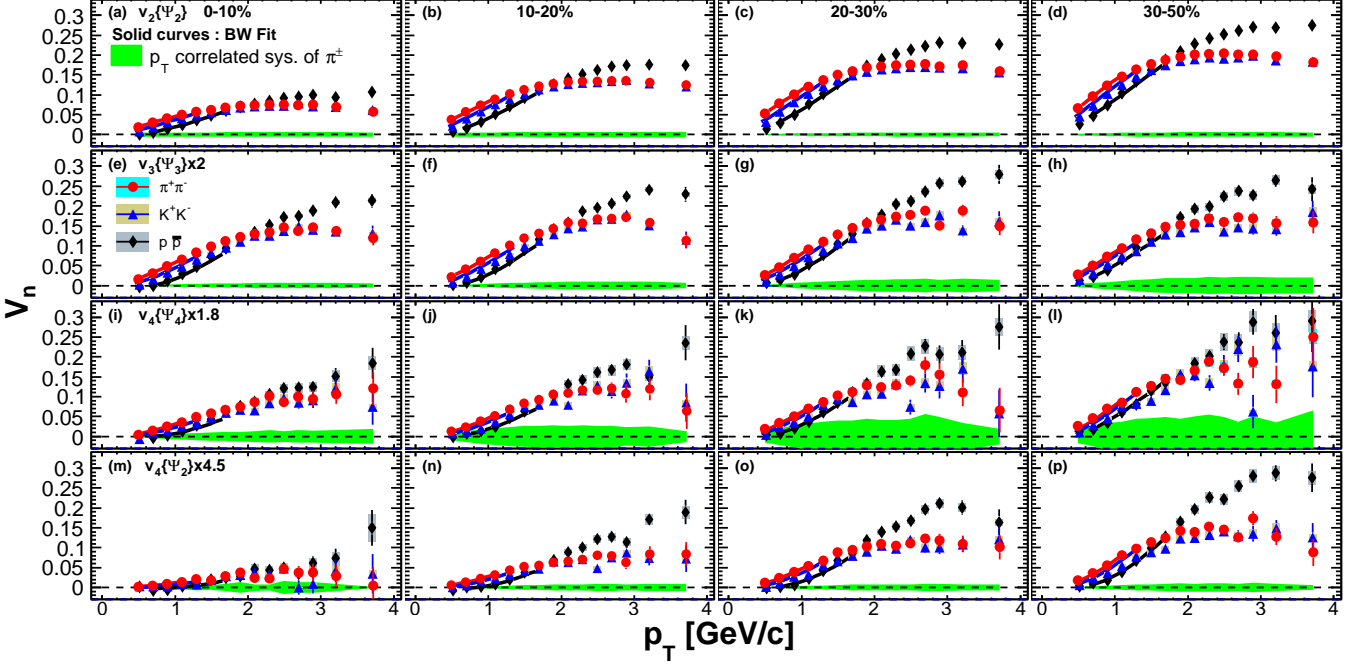


FIG. 2: (Color online) Fourier coefficients for charge combined  $\pi^\pm$ ,  $K^\pm$ , and  $p + \bar{p}$  at midrapidity in Au+Au collisions at  $\sqrt{s_{NN}} = 200$  GeV. Coefficients are determined using the event plane method. The curves illustrate the fits from the Blast-Wave model. Systematic uncertainties are shown as in Fig. 1.

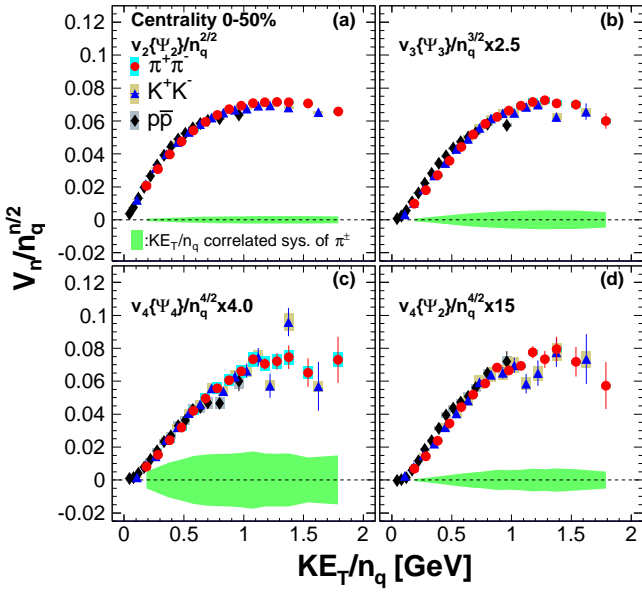


FIG. 3: (Color online) Quark-number ( $n_q$ ) scaling for 0%-50% central Au+Au collisions at  $\sqrt{s_{NN}} = 200$  GeV, where  $n_q$  is the constituent valence quark number of each hadron. Systematic uncertainties are shown as in Fig. 1.

initial-state geometric moments and converts to sizable anisotropic flow at freeze-out.

In summary, the anisotropy strengths  $v_2$ ,  $v_3$ ,  $v_4$ , and

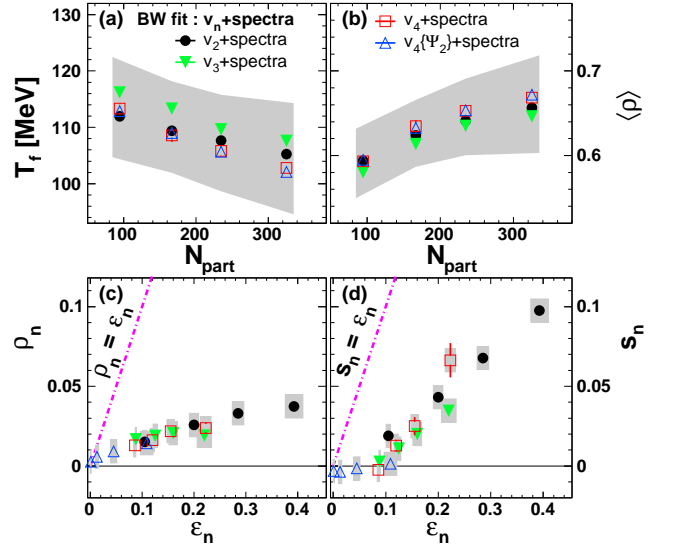


FIG. 4: (Color online) Blast Wave model fit parameters extracted at each order  $n$  across different centrality classes. The gray bands in (a)-(b) and shaded boxes in (c)-(d) indicate systematic uncertainties on the fitting  $KE_T$  range and those propagated from the measurements. Systematic uncertainties in (a) and (b) are similar among different fittings.

$v_4\{\Psi_2\}$  for  $\pi^\pm$ ,  $K^\pm$ , and  $p + \bar{p}$  produced at midrapidity in Au+Au collisions at RHIC have been presented. The higher-order harmonics  $v_n$  show particle mass splitting at

low  $p_T$  and baryon-meson difference at intermediate  $p_T$  very similar to what has been seen already for  $v_2$ . The anisotropies obey a modified quark number scaling where  $v_n/(n_q)^{n/2}$  falls on a common trend against  $\text{KE}_T/n_q$  for each  $n$ , which can be taken as an indication of hydrodynamic expansion, a quark coalescence process, and/or an acoustic nature of the QGP. The data can constrain a generalized Blast Wave model with anisotropies in radial rapidity and spatial density at higher harmonic orders, providing a geometrical and dynamical view of the hydrodynamical expansion at the end of freeze-out. Combined analysis with HBT and jet-like correlations with respect to higher order event planes will further constrain the conditions and properties of the matter created at RHIC.

We thank the staff of the Collider-Accelerator and Physics Departments at Brookhaven National Laboratory and the staff of the other PHENIX participating institutions for their vital contributions. We acknowledge support from the Office of Nuclear Physics in the Office of Science of the Department of Energy, the National Science Foundation, Abilene Christian University Research Council, Research Foundation of SUNY, and Dean of the College of Arts and Sciences, Vanderbilt University (U.S.A), Ministry of Education, Culture, Sports, Science, and Technology and the Japan Society for the Promotion of Science (Japan), Conselho Nacional de Desenvolvimento Científico e Tecnológico and Fundação de Amparo à Pesquisa do Estado de São Paulo (Brazil), Natural Science Foundation of China (P. R. China), Ministry of Education, Youth and Sports (Czech Republic), Centre National de la Recherche Scientifique, Commissariat à l'Énergie Atomique, and Institut National de Physique Nucléaire et de Physique des Particules (France), Bundesministerium für Bildung und Forschung, Deutscher Akademischer Austausch Dienst, and Alexander von Humboldt Stiftung (Germany), Hungarian National Science Fund, OTKA (Hungary), Department of Atomic Energy and Department of Science and Technology (India), Israel Science Foundation (Israel), Basic Science Research Program through NRF of the Ministry of Education (Korea), Physics Department, Lahore University of Management Sciences (Pakistan), Ministry of Education and Science, Russian Academy of Sciences, Federal Agency of Atomic Energy (Russia), VR and Wallenberg Foundation (Sweden), the U.S. Civilian Research and Development Foundation for the Independent States of the Former Soviet Union, the US-Hungarian Fulbright Foundation for Educational Exchange, and the US-Israel Binational Science Foundation.

- [1] E. V. Shuryak, CERN-83-01.
- [2] I. Arsene *et al.* (BRAHMS Collaboration), Nucl. Phys. A **757**, 1 (2005).
- [3] B. B. Back *et al.* (PHOBOS Collaboration), Nucl. Phys. A **757**, 28 (2005).
- [4] J. Adams *et al.* (STAR Collaboration), Nucl. Phys. A **757**, 102 (2005).
- [5] K. Adcox *et al.* (PHENIX Collaboration), Nucl. Phys. A **757**, 184 (2005).
- [6] H. Song *et al.*, Phys. Rev. Lett. **106**, 192301 (2011).
- [7] G. S. Denicol, T. Kodama, and T. Koide, arXiv:1002.2394.
- [8] B. Schenke, S. Jeon, and C. Gale, Phys. Rev. C **85**, 024901 (2012).
- [9] J.-Y. Ollitrault, Phys. Rev. D **46**, 229 (1992).
- [10] A. Adare *et al.* (PHENIX Collaboration), Phys. Rev. Lett. **105**, 062301 (2010).
- [11] A. Adare *et al.* (PHENIX Collaboration), Phys. Rev. Lett. **107**, 252301 (2011).
- [12] K. Aamodt *et al.* (ALICE Collaboration), Phys. Rev. Lett. **107**, 032301 (2011).
- [13] G. Aad *et al.* (ATLAS Collaboration), Phys. Rev. C **86**, 014907 (2012).
- [14] S. Chatrchyan *et al.* (CMS Collaboration), Eur. Phys. J. C **72**, 2012 (2012).
- [15] L. Adamczyk *et al.* (STAR Collaboration), Phys. Rev. C **88**, 014904 (2013).
- [16] B. Alver and G. Roland, Phys. Rev. C **81**, 054905 (2010).
- [17] R. A. Lacey, A. Taranenko, N. N. Ajitanand, and J. M. Alexander, arXiv:1105.3782.
- [18] F. G. Gardim, F. Grassi, M. Luzum, and J.-Y. Ollitrault, Phys. Rev. Lett. **109**, 202302 (2012).
- [19] S. Plumari, V. Greco, and L. P. Csernai, arXiv:1304.6566.
- [20] V. Greco, C. M. Ko, and P. Lévai, Phys. Rev. Lett. **90**, 202302 (2003).
- [21] R. J. Fries, B. Müller, C. Nonaka, and S. A. Bass, Phys. Rev. Lett. **90**, 202303 (2003).
- [22] D. Molnár and S. A. Voloshin, Phys. Rev. Lett. **91**, 092301 (2003).
- [23] A. Adare *et al.* (PHENIX Collaboration), Phys. Rev. Lett. **98**, 162301 (2007).
- [24] A. Adare *et al.* (PHENIX Collaboration), submitted to arXiv and to Phys. Rev. C.
- [25] E. Schnedermann, J. Sollfrank, and U. W. Heinz, Phys. Rev. C **48**, 2462 (1993).
- [26] P. Huovinen, P. F. Kolb, U. W. Heinz, P. V. Ruuskanen, and S. A. Voloshin, Phys. Lett. B **503**, 58 (2001).
- [27] C. Adler *et al.* (STAR Collaboration), Phys. Rev. Lett. **87**, 182301 (2001).
- [28] K. Adcox *et al.* (PHENIX Collaboration), Nucl. Instrum. Methods Phys. Res., Sect. A **499**, 469 (2003).
- [29] K. Adcox *et al.* (PHENIX Collaboration), Nucl. Instrum. Methods Phys. Res., Sect. A **499**, 489 (2003).
- [30] A. Adare *et al.* (PHENIX Collaboration), Phys. Rev. C **85**, 064914 (2012).
- [31] E. Richardson *et al.* (PHENIX Collaboration), Nucl. Instrum. Methods Phys. Res., Sect. A **636**, 99 (2011).
- [32] S. Afanasiev *et al.* (PHENIX Collaboration), Phys. Rev. C **80**, 024909 (2009).
- [33] A. M. Poskanzer and S. A. Voloshin, Phys. Rev. C **58**, 1671 (1998).
- [34] T. Todoroki and T. Niida, Doctoral Theses at the University of Tsukuba (2014), <http://www.phenix.bnl.gov/WWW/talk/theses.php>.

\* Deceased

† PHENIX Co-Spokesperson: morrison@bnl.gov

‡ PHENIX Co-Spokesperson: jamie.nagle@colorado.edu

- [35] R. A. Lacey (PHENIX Collaboration), Nucl. Phys. A **698**, 559 (2002).
- [36] K. Adcox *et al.* (PHENIX Collaboration), Phys. Rev. Lett. **89**, 212301 (2002).
- [37] H. Masui and A. Schmah, arXiv:1212.3650.
- [38] G. Aad *et al.* (ATLAS Collaboration), arXiv:1403.0489.
- [39] M. Luzum, C. Gombeaud, and J.-Y. Ollitrault, Phys. Rev. C **81**, 054910 (2010).
- [40] N. Borghini and J.-Y. Ollitrault, Phys. Lett. B **642**, 227 (2006).
- [41] P. F. Kolb, L.-W. Chen, V. Greco, and C. M. Ko, Phys. Rev. C **69**, 051901 (2004).
- [42] S. S. Adler *et al.* (PHENIX Collaboration), Phys. Rev. C **69**, 034909 (2004).
- [43] S. S. Adler *et al.* (PHENIX Collaboration), Phys. Rev. C **72**, 014903 (2005).
- [44] M. L. Miller, K. Reygers, S. J. Sanders, and P. Steinberg, Ann. Rev. Nucl. Part. Sci. **57**, 205 (2007).